

Supporting Information

A novel rechargeable aqueous bismuth-air battery

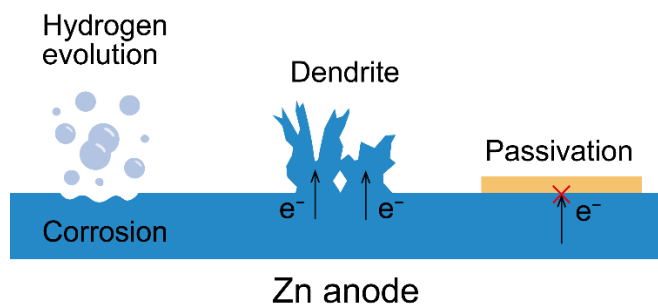


Figure S1. Scheme of repeated plating/stripping on Zn anode. The Zn anode suffers from a poor cycling stability in aqueous electrolytes due to H_2 evolution reaction, passivation layer formation (such as zinc hydroxides and zincates), and Zn dendrite growth.

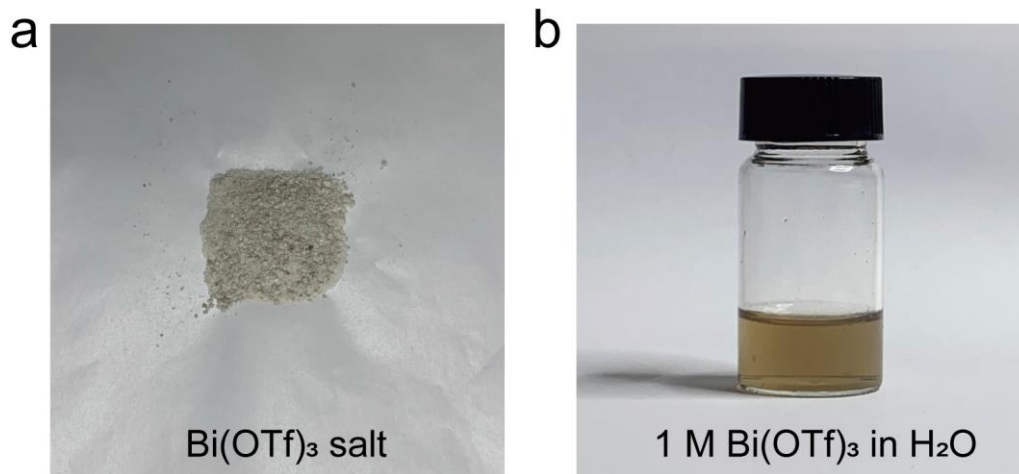


Figure S2. Photographs of (a) Bi(OTf)₃ salt and (b) 1 M Bi(OTf)₃ aqueous electrolyte.



Figure S3. The pH of 1 M Bi(OTf)₃ aqueous electrolyte.

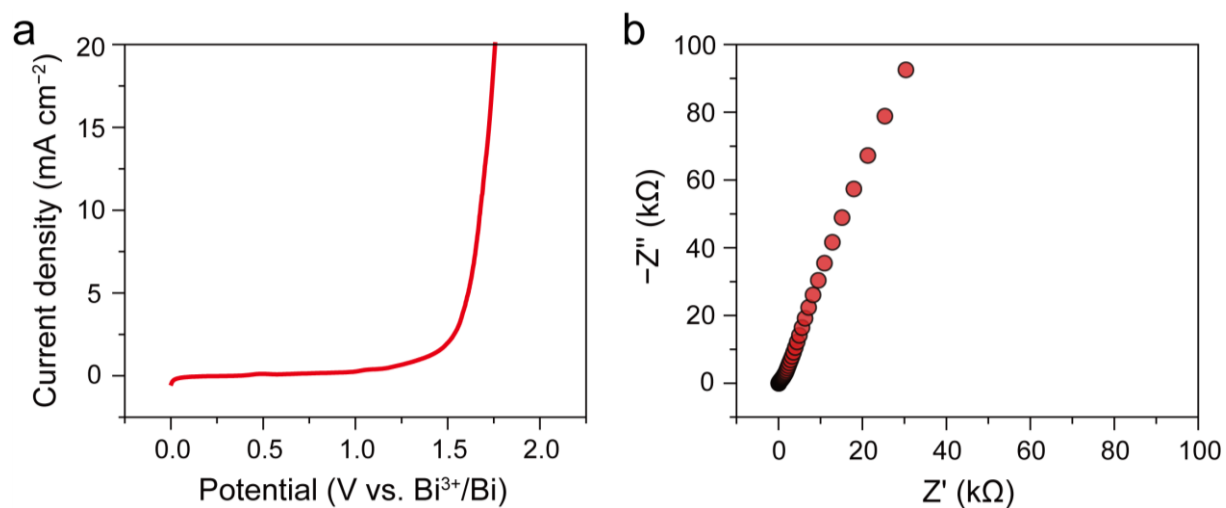


Figure S4. (a) Electrochemical stability window and (b) ionic conductivity of the 1 M Bi(OTf)₃ electrolyte. The ionic conductivity was calculated from $\sigma = l / (R_b \times A)$ where σ is the ionic conductivity (S cm⁻¹), l is the thickness (0.5 cm), A is the area (1 cm²), and R_b (Ω) is the bulk resistance in impedance spectroscopy.

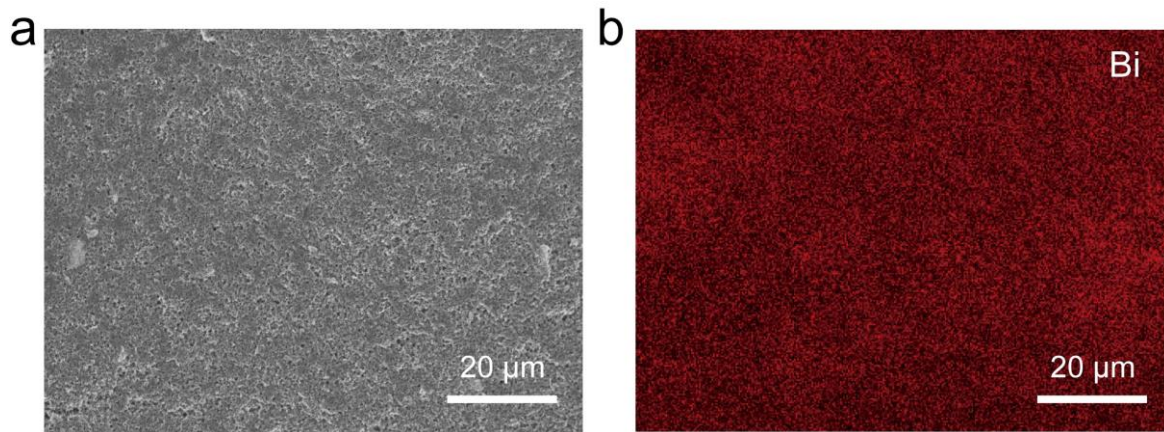


Figure S5. (a) SEM image and (b) the corresponding element mapping of Bi anode.

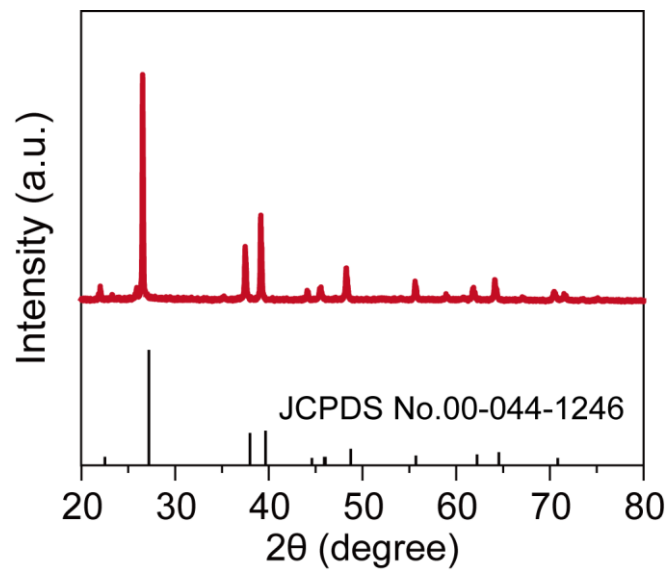


Figure S6. XRD pattern of Bi anode.

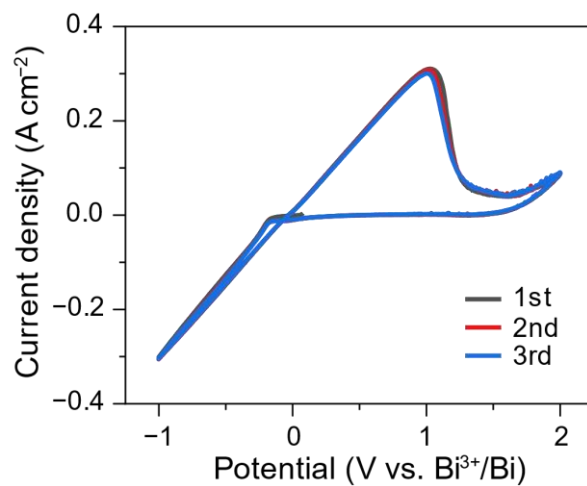


Figure S7. CV curves at a scan rate of 10 mV s^{-1} in a three-electrode cell using 1 M Bi(OTf)_3 electrolyte. Carbon paper was used as working electrode, and Bi metal plates were used as counter electrode and reference electrode.

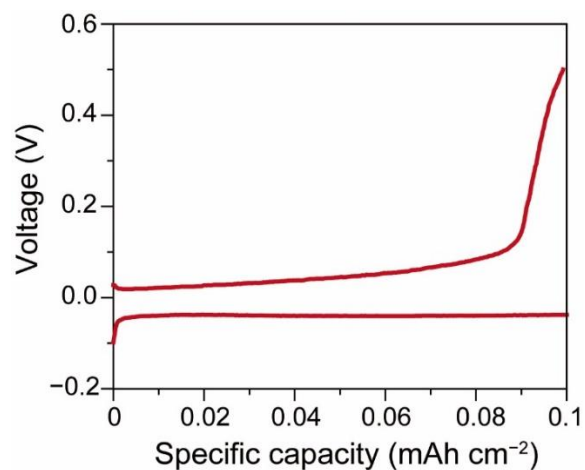


Figure S8. Voltage profiles of the C||Bi cells using the Bi(OTf)₃ electrolyte at 0.1 mA cm⁻² with the capacity of 0.1 mAh cm⁻² and cut-off voltage of 0.5 V.

The specific capacity of Bi anode

$$\begin{aligned}
 &= \frac{\text{stripped capacity of bismuth anode}}{\text{the mass of plated bismuth}} \\
 &= \frac{\text{stripped capacity of bismuth anode}}{\text{plated capacity bismuth}} \times \text{theoretical specific capacity of bismuth} \\
 &= \frac{0.0996}{0.1} \times 385 \text{ mAh g}^{-1} = 383 \text{ mAh g}^{-1}
 \end{aligned}$$

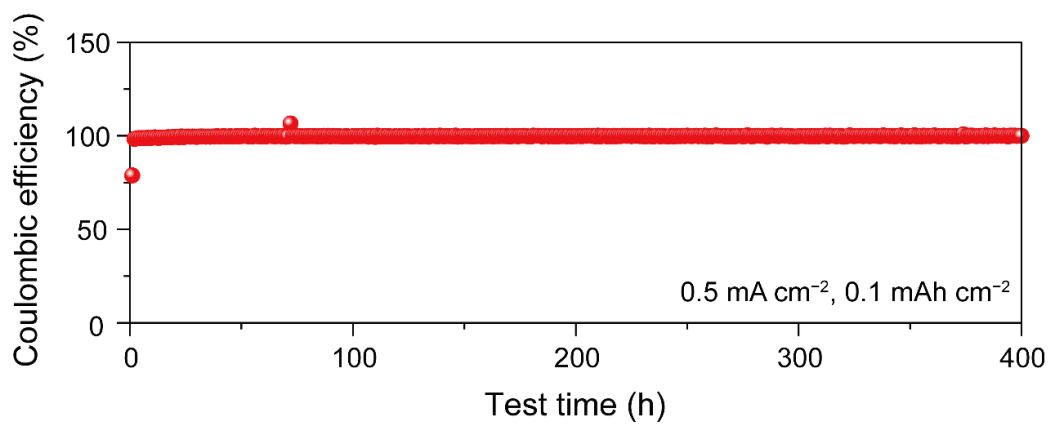


Figure S9. Coulombic efficiency of C||Bi cells using the Bi(OTf)₃ electrolyte at 0.5 mA cm⁻² with the capacity of 0.1 mAh cm⁻² and the cut-off voltage of 0.5 V.

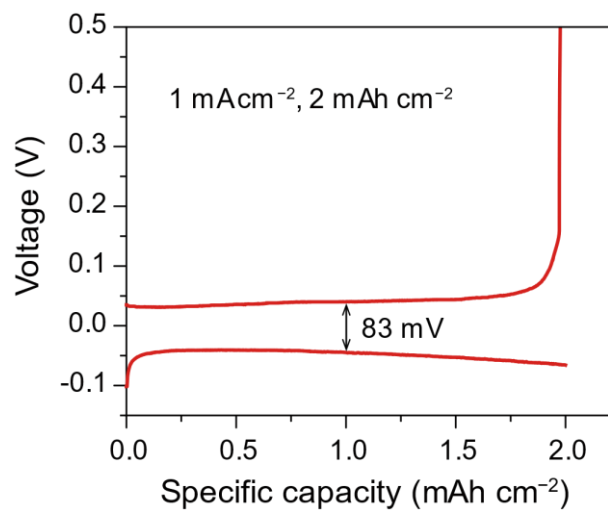


Figure S10. Voltage profile of the C||Bi cell using the Bi(OTf)₃ electrolyte at 1 mA cm⁻² with the capacity of 2 mAh cm⁻².

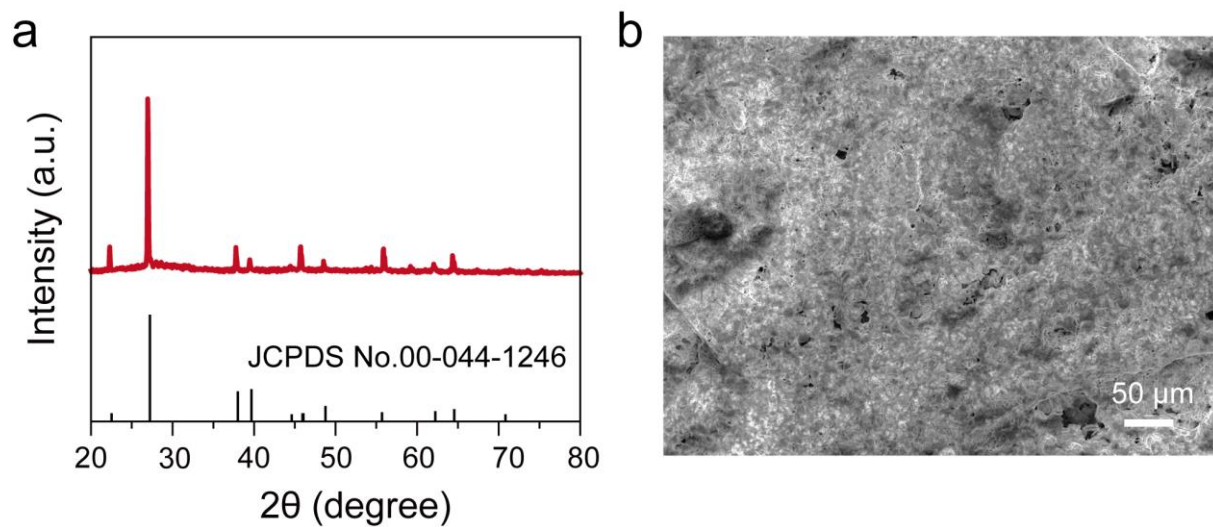


Figure S11. (a) XRD pattern and (b) SEM image of Bi electrode extracted from Bi symmetric cells using 1 M $\text{Bi}(\text{OTf})_3$ aqueous electrolyte after 100 cycles at 1 mA cm^{-2} and 0.5 mAh cm^{-2} .

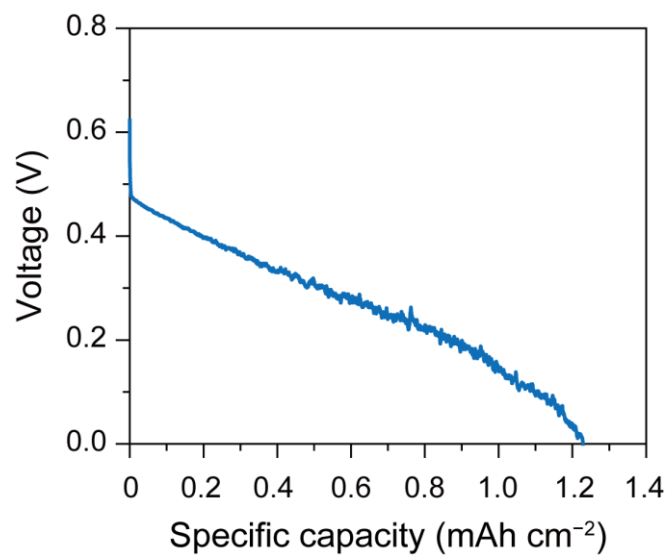


Figure S12. The galvanostatic discharge profile of Bi-air batteries using 6 M KOH electrolyte at 0.1 mA cm⁻² with the cut-off voltage of 0 V.

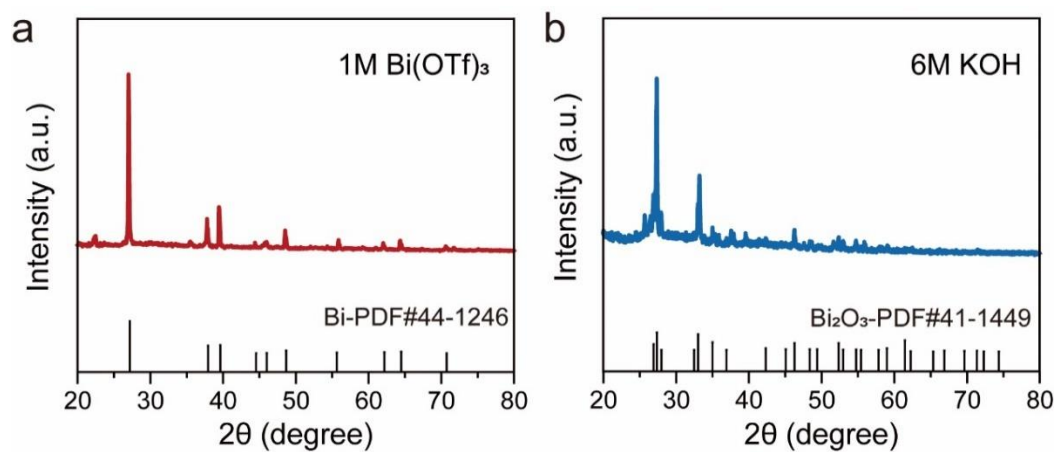


Figure S13. XRD patterns of Bi anode after immersed in 1 M $\text{Bi}(\text{OTf})_3$ aqueous electrolyte and 6 M KOH aqueous solution for 12 h.

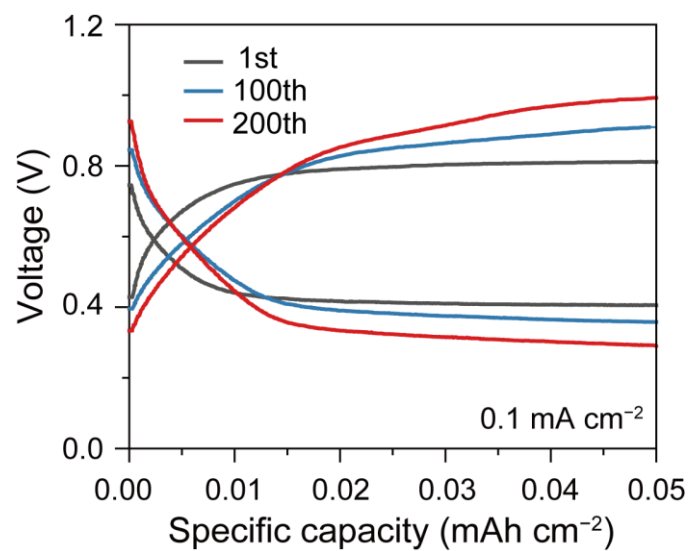


Figure S14. The galvanostatic discharge/charge profiles of Bi-air battery at a current density of 0.1 mA cm^{-2} with the capacity of 0.05 mAh cm^{-2} .

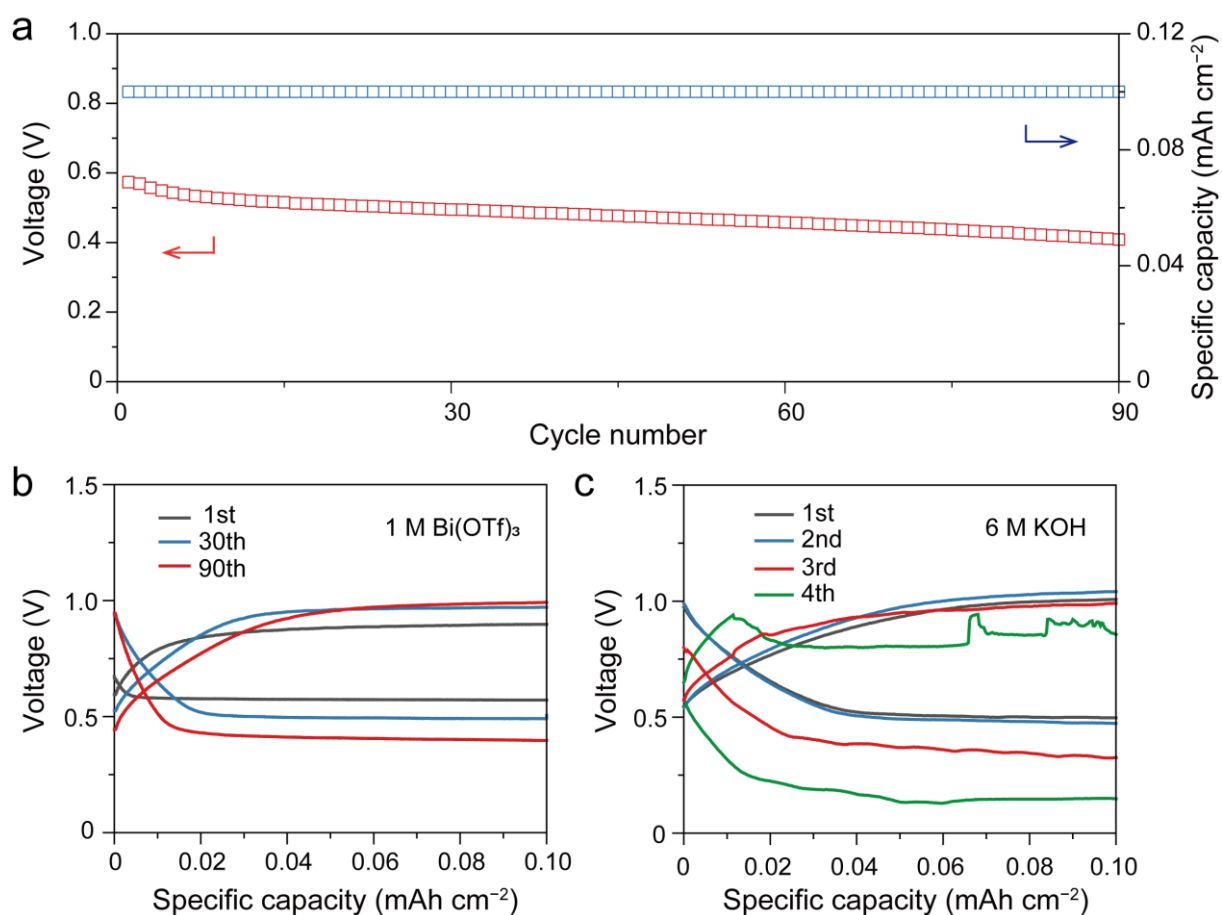


Figure S15. (a) Cycling performance of Bi-air battery using 1 M Bi(OTf)₃ electrolyte at the current density of 0.1 mA cm⁻² with the capacity of 0.1 mAh cm⁻². (b) The corresponding discharge/charge profiles of Bi-air battery. (c) The galvanostatic discharge/charge profiles of Bi-air battery using 6 M KOH electrolyte at the current density of 0.1 mA cm⁻² with the capacity of 0.1 mAh cm⁻².

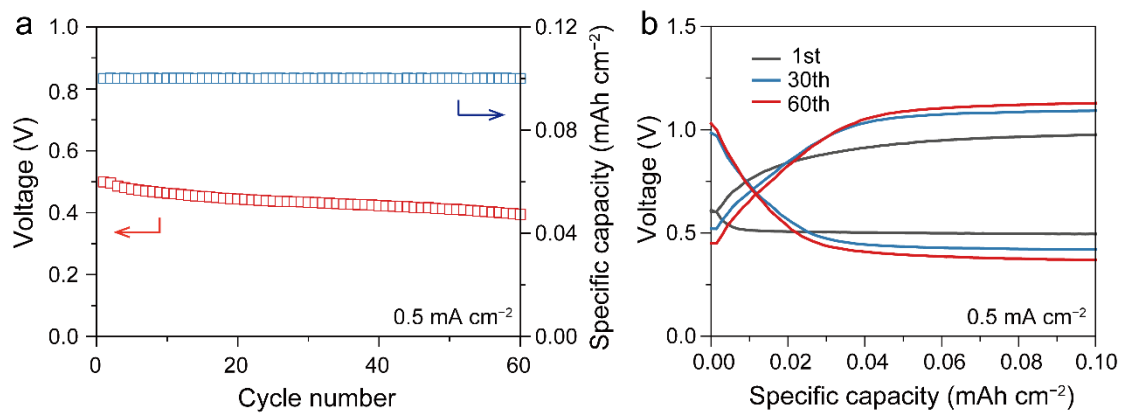


Figure S16. (a) Cycling performance of Bi-air battery using 1 M Bi(OTf)₃ electrolyte at the current density of 0.5 mA cm⁻² with the capacity of 0.1 mAh cm⁻². (b) The corresponding discharge/charge curves of Bi-air battery.

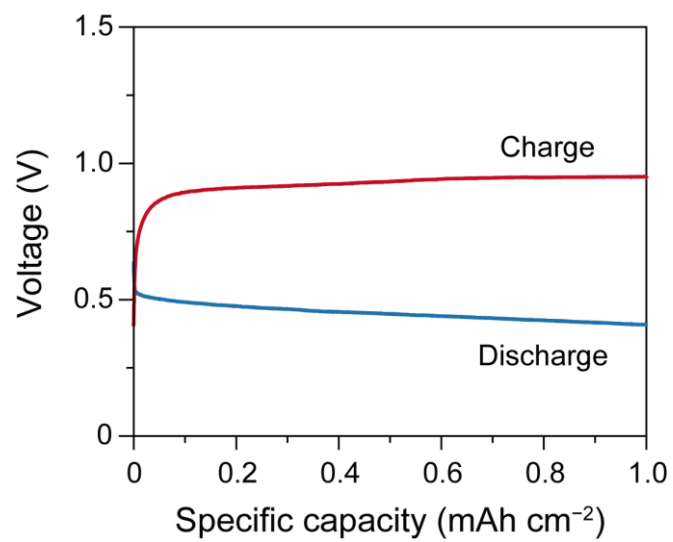


Figure S17. Discharge/charge profiles of Bi-air batteries using Bi(OTf)₃ electrolyte at 0.1 mA cm⁻² with the capacity of 1 mAh cm⁻².

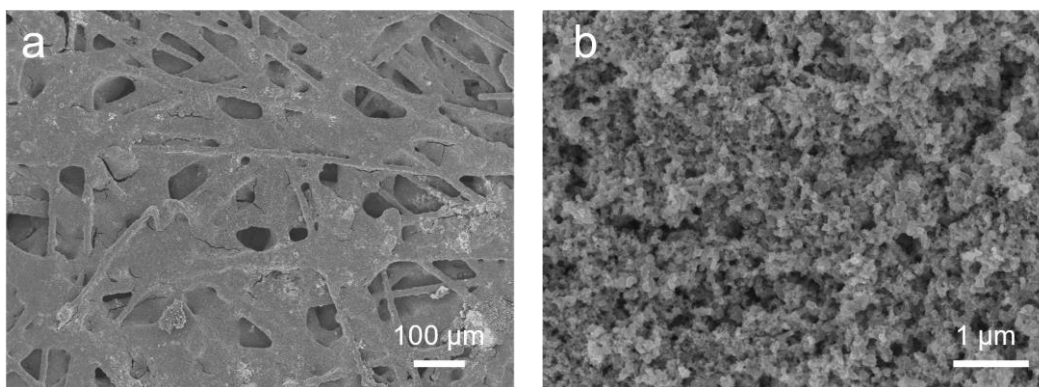


Figure S18. SEM images of pristine air cathode with the loading of 1 mg cm^{-2} Pt/C catalyst.

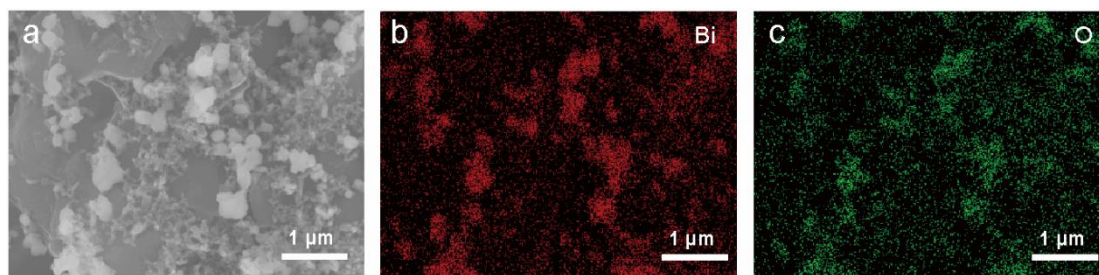


Figure S19. (a) SEM image and (b) corresponding elemental mappings of discharged air cathode.

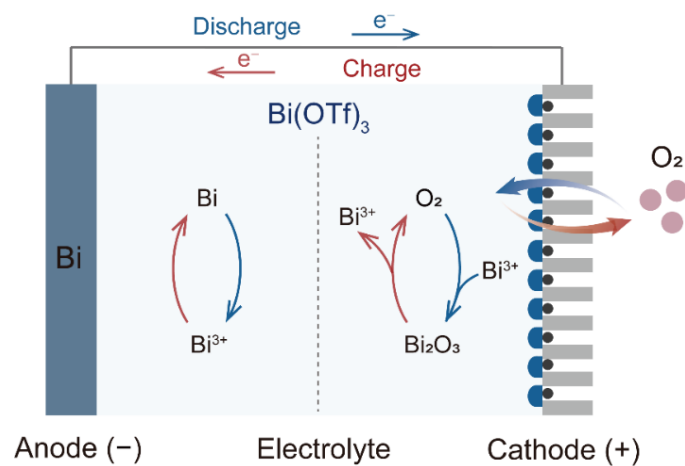
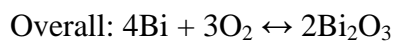
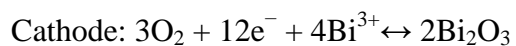
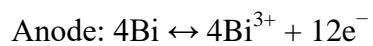


Figure S20. Schematic of the electrically rechargeable Bi-air battery using $\text{Bi}(\text{OTf})_3$ electrolyte.



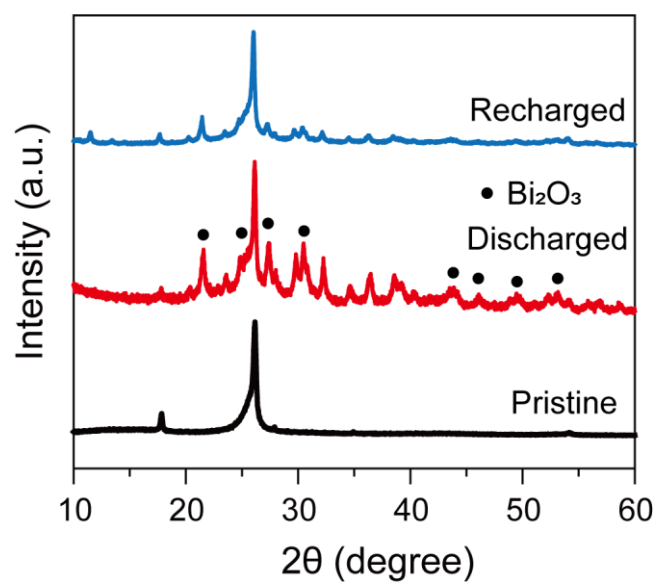


Figure S21. XRD patterns of air cathode extracted from Bi-air batteries after 200th discharge-charge process at the current density of 0.1 mA cm⁻² with the capacity of 0.05 mAh cm⁻².

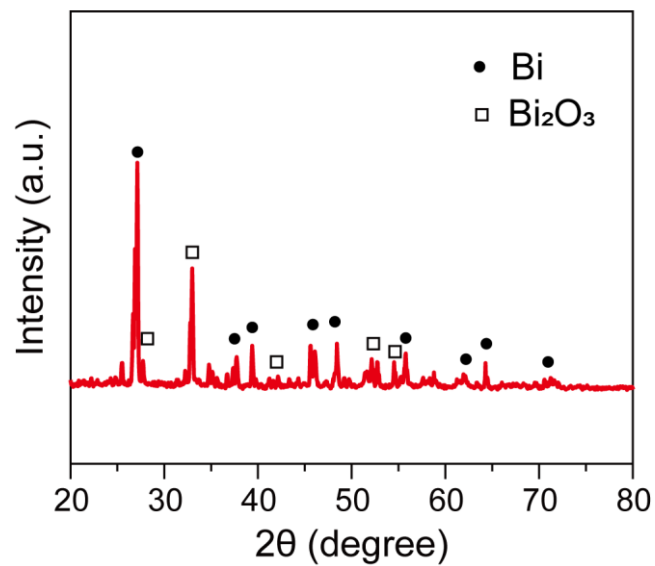


Figure S22. XRD pattern of Bi anode extracted from Bi-air batteries after 200th discharge-charge process at the current density of 0.1 mA cm^{-2} with the capacity of 0.05 mAh cm^{-2} .